Available online at www.sciencedirect.com
SCIENCE DIRECT®
International Journal of Heat and Mass Transfer 47 (2004) 2085–2096
International Journal of HEAT and MASS TRANSFER
www.elsevier.com/locate/ijhmt

Experimental research on convection heat transfer in sintered porous plate channels

Pei-Xue Jiang [a,*], Meng Li [a], Tian-Jian Lu [b], Lei Yu [a], Ze-Pei Ren [a]

[a] Department of Thermal Engineering, Tsinghua University, Beijing 100084, China
[b] Department of Engineering, University of Cambridge, Cambridge, CB2 1PZ, UK

Received 5 June 2003; received in revised form 11 December 2003

Abstract

Forced convection heat transfer of water and air in sintered porous plate channels was investigated experimentally. The effects of fluid velocity, particle diameter, type of porous media (sintered or non-sintered), and fluid properties on the convection heat transfer and heat transfer enhancement were investigated. The results showed that the convection heat transfer in the sintered porous plate channel was more intense than in the non-sintered porous plate channel due to the reduced thermal contact resistance and the reduced porosity near the wall in the sintered material, especially for convection heat transfer of air. For the tested conditions, the local heat transfer coefficients in the sintered porous plate channels were increased up to 15 times for water and 30 times for air. The heat transfer enhancement due to the sintered porous media with air intensified sharply with increasing flow rate. However, the influence of particle diameter on the convection heat transfer in the sintered porous media was not great. The effective thermal conductivity of the sintered porous media was found to be much higher than for non-sintered porous media due to the improved thermal contact caused by the sintering process.

Keywords: Porous media; Experimental research; Convection heat transfer; Heat transfer enhancement; Sintered

1. Introduction

Porous media intensify fluid flow mixing and increase the surface area in contact with the coolant, so porous structures are an effective heat transfer augmentation technique. Heat transfer in porous media has received much attention for many years due to its importance in applications such as catalytic and chemical particle beds, solid matrix or micro-porous heat exchangers, cooling of electronic equipment and mirrors in powerful lasers, phased-array radar systems, industrial furnaces, packed-bed regenerators, combustors, fixed-bed nuclear propulsion systems, micro-thrusters, transpiration cooling, spacecraft thermal management systems, and many others [1–5].

Jeigarnik et al. [2] experimentally investigated convection heat transfer of water on flat plates and in channels filled with porous material such as sintered spherical particles, nets, porous metal, and felts. Most of their experimental data was for convection heat transfer in sintered bronze porous layers with different thickness (0.86–3.9 mm) and particle diameters (0.1–0.6 mm). They found that the porous media increased the heat transfer coefficient 5–10 times although the hydraulic resistance was increased even more. Lage et al. [3] studied a low permeability microprobe heat sink for cooling phased-array radar systems. Their results suggested that an increased overall heat transfer coefficient could be obtained that would reduce the operational temperature of the electronics for the same waste heat generation rate. Hwang and Chao [6] experimentally and numerically studied convection heat transfer of air

* Corresponding author. Tel.: +86-10-6277-2661; fax: +86-10-6277-0209.
E-mail address: jiangpx@te.tsinghua.edu.cn (P.-X. Jiang).

0017-9310/$ - see front matter © 2004 Elsevier Ltd. All rights reserved.
doi:10.1016/j.ijheatmasstransfer.2003.12.004

Nomenclature

c_{pf}	fluid specific heat, J/(kg K)
d_p	particle diameter, m
D_e	porous plate channel hydraulic diameter, m
f_e	friction factor
h	average heat transfer coefficient, W/(m^2 K)
h_c	channel height, m
h_x	local heat transfer coefficient, W/(m^2 K)
L	channel length, m
M	mass flux, ($=\rho u$), kg/(m^{2}s)
M_t	total weight of sintered porous plate, kg
Nu	Nusselt number
Δp	pressure drop, Pa
Pr	Prandtl number
q	heat flux, W/m^2
Re_D	Reynolds number based on the plate channel hydraulic diameter, ($=\rho_f u_f D_e/\mu_f$)
Re_e	equivalent Reynolds number, ($=2Md_p/(3\mu_f(1-\varepsilon))$)
t	temperature, °C
Δt	temperature difference, °C
u	fluid velocity in the x direction, m/s
w_p	sintered porous plate width, m
x, y	coordinates, m

Greek symbols

λ	thermal conductivity, W/(m K)
μ_f	fluid absolute viscosity, Ns/m^2
ρ	fluid density, kg/m^3
ε_m	mean porosity
σ_t	total thickness of sintered porous plate, m
σ_c	copper plate thickness, m

Subscripts

0	heated section inlet
c	copper
f	fluid
l	lower
m	mean or effective
p	particle
u	upper
w	wall
x	local

in 5×5×1 cm sintered porous channels. They showed that the porous channels can be used as a heat sink for high-performance forced air cooling in micro-electronics. With a porous heat sink having $d_p = 0.72$ mm, the forced air heat transfer coefficient was increased from 100 to 5000 W/(m^2 K). They also showed that the conventional thermal equilibrium one-equation model overpredicts the Nusselt number for sintered porous channel flow. Jiang et al. [7–9] experimentally and numerically studied convection heat transfer of water or air in non-sintered porous (packed beds) plate channels which showed that the packed beds greatly intensified the convection heat transfer (up to 10-fold). A modified criterion was then developed to describe the effect of particle diameter on the heat transfer coefficient [8]. Khanafer and Vafai [10] presented an innovative way to produce and regulate an isothermal surface in high heat flux applications through the use of two basic configurations with variable area porous channels.

There have been numerous investigations with theoretical analyses and numerical simulations of convection heat transfer in fluid-saturated porous media. Vafai and Tien [11] investigated the nature and importance of the boundary and inertial effects upon the flow and heat transfer in porous media. They showed that the boundary effects have very little effect on the overall flow field. However, the boundary have a significant effect on the heat transfer. The inertial effects increase with higher permeability and the lower fluid viscosity. The velocity gradients near the wall are bound to increase, thereby increasing the viscous resistance due to the boundary. Narasimhan et al. [12,13] presented a new theory for predicting the thermo-hydraulic effect on fully developed convection by a fluid with temperature-dependent viscosity flowing through a porous medium channel. The theory incorporates the form-drag effect of the porous medium by invoking the differential representation of the Hazen–Dupuit–Darcy (HDD) equation. The theoretical predictions were compared with results from a simpler linear (Darcy) model and with numerical results simulating the operation of a realistic porous medium enhanced cold-plate and were verified with experiments. The comparisons showed that the second-order HDD model predictions agreed well with the hydraulic simulation results and the experimental results for all of the heat flux values tested.

In theoretical and numerical investigations of convection heat transfer in porous media, two different models have been used for the energy equation: the local thermal equilibrium model and the local thermal non-equilibrium model. In recent years the local thermal non-equilibrium model has been used more frequently in the energy equation in theoretical and numerical research on convection heat transfer in porous media [6,7,9–19]. With the thermal non-equilibrium model, the treatment of the boundary conditions for the energy equation significantly affects the numerical results. A number of papers have analyzed this problem, e.g.

[9,14–19]. Alazmi and Vafai [19] analyzed eight different forms of constant wall heat flux boundary conditions in the absence of local thermal equilibrium conditions in the porous media. They showed that different boundary conditions may lead to substantially different results. In addition, they pointed out that selecting one model over the others is not an easy issue since previous studies validated each of the two primary models and because the mechanics of splitting the heat flux between the two phases is not yet resolved.

Jiang et al. [14] numerically investigated forced convection heat transfer in plate channels filled with non-sintered metallic or non-metallic particles or sintered porous media using a non-thermal equilibrium model. Their numerical simulation results were compared with experimental data from Jiang et al. [8,9] and Hwang et al. [6] to analyze the effects of the assumed boundary conditions. The analysis investigated the difference in the convection heat transfer in packed beds or in sintered porous media and the effects of the boundary condition assumptions. The results showed that the numerical simulation of convection heat transfer of air and water in non-sintered packed beds using a local thermal non-equilibrium model with the assumption of equal heat fluxes from the heat transfer surface into the solid and the fluid agreed best with the experimental data. However, for sintered porous media numerical simulations showed that the boundary conditions at the wall should be that the particles temperatures are equal to the fluid temperature. In addition, the convection heat transfer coefficient in sintered porous media is much higher than that in packed beds. These results need further clarification with additional experimental data.

The convection heat transfer in porous media has been widely investigated experimentally and theoretically; however, the difference between the convection heat transfer in sintered and non-sintered porous media was not investigated systematically. The mathematical model for convection heat transfer in porous media still needs to be improved which will require extensive experimental data. The present work experimentally studied forced convection heat transfer of water or air in plate channels filled with sintered bronze particles. The study investigated the effects of the fluid type, the flow velocity, the particle diameter and the type of porous media (sintered or non-sintered) on the convection heat transfer. Research on convection heat transfer in sintered porous media has practical importance for improving and analyzing some important technologies such as transpiration cooling, micro-porous heat exchangers and micro-thrusters which use sintered metallic porous structures. The experimental data was also used to clarify the mathematical model and numerical results for convection heat transfer in sintered porous media.

2. Experimental system and data reduction

The experimental systems used to investigate convection heat transfer of water and air in porous media are shown schematically in Fig. 1. The water system included a water tank, a pump, a constant water head tank, a test section, a heat exchanger, a data acquisition system (Keithley 2000), pressure gauges, thermocouples and an electrical power input and measurement system. The constant water head tank was especially useful when verifying the accuracy of the experimental system for an empty plate channel with small mass flow rates. The system used to investigate convection heat transfer of air in porous media included a compressor, a test section, two volumetric flow meters, a data acquisition system (Keithley 2700), pressure gauges, thermocouples and an electrical power input and measurement system.

The test section enclosure that sealed the test section was made from stainless steel plates. The sintered porous channel was made of bronze particles sintered to a thin copper plate which was placed in the stainless steel channel. The test section is shown in Fig. 2. The upper copper plate of the test section was 1.0 mm thick. The sintered bronze material was 89/11 copper/tin mix with a typical 0.3% phosphorous content. The nominal particle sizes of the sintered porous plates were 0.5–0.71, 1–1.4 and 1.4–2 mm. The length and width of the sintered porous plates were 210 and 120 mm, and the thicknesses of the three sintered porous plates were 11.73, 10.87 and 10.22 mm. The porosities of the sintered porous plates were 0.402, 0.444 and 0.463. The upper copper plate on the channel received a constant heat flux, q_w, while the bottom and side plates were adiabatic. The flow entered the channel with an average velocity, u_0, and constant temperature as shown in Fig. 2.

To prevent leakage of the fluid along the contact surface between the sintered porous plate and the stainless steel channel, a thin layer of polytetrafluoroethylene (PTFE) was placed on the bottom and sides between the porous plate and the stainless steel and sealed. An electrical heater was placed on the copper plate with a heavy stainless steel cover placed on top with the four edges of the upper surface of the test section sealed with a silicon–rubber sealing pad. The top was then tightened down with screws. Many tests showed that the leakage was very small even for relatively high pressures (e.g. 6 bar). The test section and most of the tubes including the inlet and outlet measurement sections were insulated using silicate glass fiber and sponges.

The heater was manufactured by wire machining a 0.1 mm thickness nickel–chromium sheet (Cr20 Ni80) into a continuous serpentine strip. The strip was mounted on a thermally conductive rubber pad (boron oxide, JS-T500) having a thermal conductivity of 2.05 W/(m K) as an insulator which could sustain 4000 V.

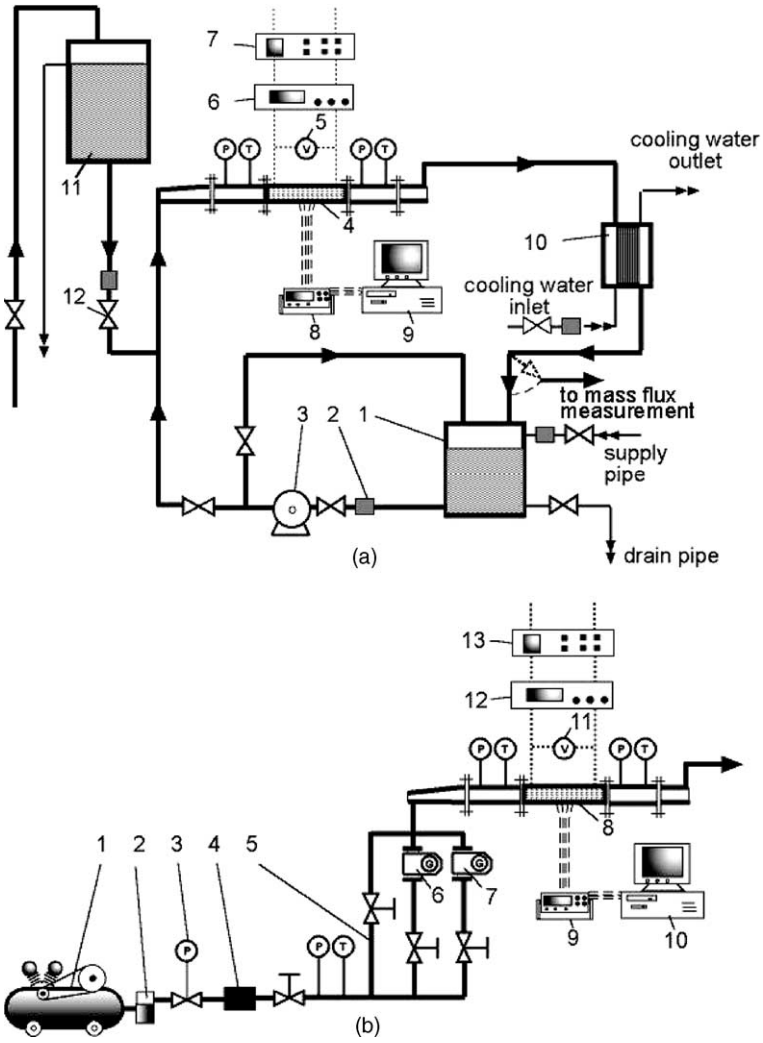

Fig. 1. Experimental apparatus for heat transfer of water (a) and air (b) in porous media. (a) 1: water tank, 2: filter, 3: pump, 4: test section, 5: voltmeter, 6: voltage regulator, 7: voltage stabilizer, 8: data acquisition system, 9: personal computer, 10: heat exchanger, 11: constant water head tank, 12: valve. (b) 1: compressor, 2: water filter, 3: pressure regulator, 4: filter, 5: by-pass, 6,7: volumetric flow meters, 8: test section, 9: data acquisition system, 10: computer, 11: voltmeter, 12: voltage regulator, 13: voltage stabilizer.

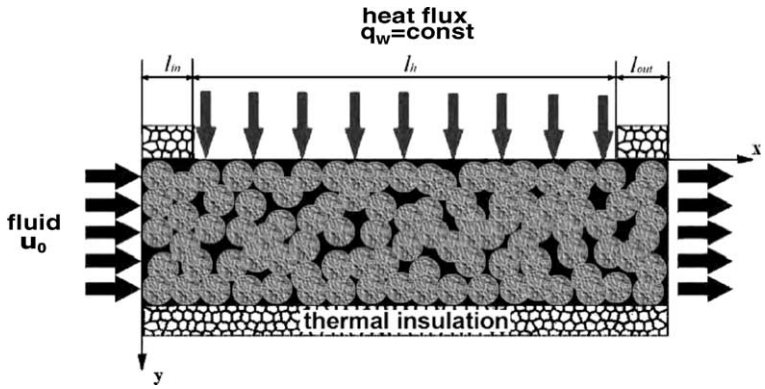

Fig. 2. Test section and schematic diagram of the physical system.

This heater worked very well and never burned out. A detailed numerical analysis showed that the heat flux on the bottom surface of the test section was sufficiently uniform when using this heater

The parameters measured in the experiments included the wall temperatures, the inlet and outlet temperatures, the working temperature and pressure of the volumetric flow meters, the inlet and outlet pressures, the flow rate and the heater voltages. The local temperature of the plate channel was measured with 25 copper–constantan thermocouples. Seventeen thermocouples were inserted into the upper plate of the test section (0.5 mm deep) along the centerline. Eight more thermocouples were inserted into the upper plate of the test section (0.5 mm deep) along a line 25 mm from the centerline to monitor the temperature variations across the test section. The inlet water temperature was measured by 2 thermocouples located at the inlet. Three thermocouples were located at the plate channel outlet after a mixer to measure the bulk exit temperature. Prior to installation, the thermocouples were calibrated using a constant-temperature oil bath. The overall accuracy was within ±0.1 °C. The inlet and outlet pressures were measured using accurate manometers with accuracies of 0.25% of the full scale range of 0.1, 0.6 and 1.6 MPa. The water mass flow rate was measured by weighing the fluid flowing from the channel for a given time period. The air volumetric flow rate was measured using two volumetric flow meters with accuracies of 1.4% of the full scale range of 0.7–7 and 4.5–45 N m^3/h. The heater voltage was measured by a digital voltmeter. The electric power input to the heater was calculated from the measured voltage readings and the heater resistance. The same measurement method was used for the convection heat transfer in the porous media and in the empty channel.

The flow rate, input power and inlet fluid temperature were fixed for each test. The thermocouples were connected to a data acquisition system (Keithley 2700) with the temperatures monitored and then recorded after steady-state conditions were reached. The flow rate, inlet and outlet fluid bulk temperatures, and voltage across the heater were also recorded. The local bulk fluid temperature at each measuring section was calculated from the inlet temperature, flow rate and power input, or from the inlet and outlet temperatures using linear interpolation. The fluid enthalpy rise was checked against the electric power input. The experimental uncertainty for the heat balance was ±5%.

The bulk porosities of the sintered porous plates were measured and computed using

$$\varepsilon = 1 - \frac{M_t - \rho_c \sigma_c w_p L}{\rho_p (\sigma_t - \sigma_c) w_p L}. \quad (1)$$

The experimental uncertainty in the porosity was estimated to be ±1.0%.

The data reduction method was similar to that used in previous experimental research on forced convection heat transfer of water in non-sintered porous plate channels [8]. Preliminary tests were performed for data calibration and error estimates. The maximum error in the flow rate was less than 0.43% for water and 2.4% for air. Steady-state was said to be reached when the deviations of the wall temperatures, the inlet and outlet temperatures were all within ±0.25 °C for 15 min. The experimental uncertainty in the convection heat transfer was mainly caused by experimental errors in the heat balance, axial thermal conduction in the copper plate test section, temperature measurement errors and the calculation of the heat transfer surface temperature. Detailed error analyses showed that the experimental uncertainties in the convection heat transfer coefficient and pressure drop were estimated to be ±11.2% and ±2.9%.

The convection heat transfer coefficients in an empty plate channel were measured before the experimental research on the convection heat transfer in the sintered porous media. The experimental setup was evaluated by comparing the results for convection heat transfer in the empty plate channel with established correlations and numerical simulations. Experimental data was obtained in the empty plate channel for laminar, turbulent and transition flow. For laminar flow ($Re_D < 2300$), the convection heat transfer in the empty plate channel was calculated numerically. The local heat transfer coefficients for turbulent and transition convection heat transfer in the empty plate channel were calculated using the formulas proposed by Petukhov et al. [20]. The standard deviation of the experimental results relative to the predictions was ±10.0%. The experimental uncertainties near the inlet and outlet were relatively large due to longitudinal thermal conduction along the test section. In general, the experimental system accuracy was well within acceptable limits for convection heat transfer tests.

3. Experimental results and discussion

3.1. Flow resistance and friction factor

Fig. 3 shows the pressure drop for water and air in the sintered porous plate channels as a function of Reynolds number based on the hydraulic diameter. During theses hydraulic tests the channel was not heated. The inlet fluid temperatures for water and air were about 16 and 21 °C. The pressure drop in the porous media greatly increased with increasing flow rate and decreasing particle diameter. Smaller particle diameters increased the contact area between particles and reduced the pore size and the porosity in the porous media. All of these factors increased the flow resistance. In the

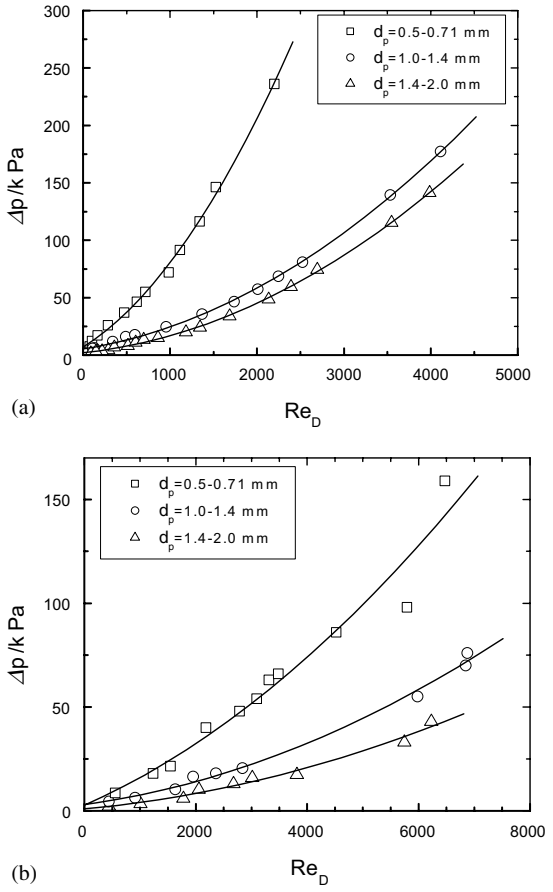

Fig. 3. Pressure drop for water (a) and air (b) in the sintered porous plate channel. □, ○, △ — experimental data.

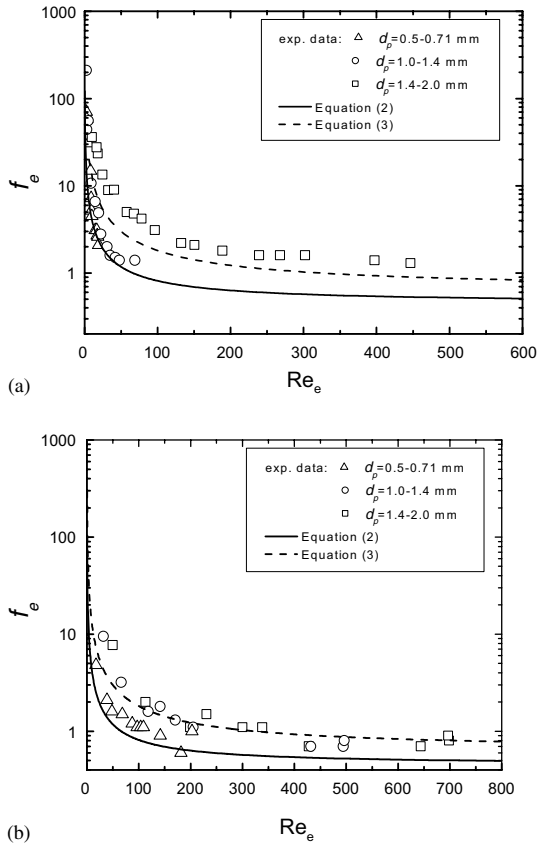

Fig. 4. Friction factors for water (a) and air (b) in the sintered porous plate channel.

experiments the air velocity was much larger than the water velocity (10 times), but the air flow resistance was less than the water flow resistance due to the lower air density.

Previous work [8] showed that the friction factor, f_e, calculated from the experimental data for fluid flow in non-sintered porous media can be well predicted using the equation given by Aerov and Tojec [21]:

$$f_e = \frac{\varepsilon_m^3}{1-\varepsilon_m}\frac{\rho_f d_p}{3M^2}\frac{\Delta p}{L} = \frac{36.4}{Re_e} + 0.45 \quad (\text{for } Re_e < 2000). \tag{2}$$

Fig. 4 compares the friction factor, f_e, calculated from the experimental data for fluid flow in the sintered porous media with the friction factor predicted using Eq. (2). The friction factors in the sintered porous plate channels decreased with decreasing particle diameter for a given Re_e. The friction factor in the sintered porous plate channel with the smallest particle diameters of 0.5–0.71 mm corresponded well with Eq. (2), while the friction factors in the sintered porous plate channels with the larger particle diameters of 1.0–1.4 and 1.4–2.0 mm were higher than predicted by Eq. (2). The increased friction factor for the porous media with larger particle diameters may result from the number of particle layers in the vertical direction decreasing with increasing particle diameter so that the porosity variation in the porous channel became sharper than that for the data used to develop Eq. (2). The increased pressure drop resulted from the sintering process changing the porous structure so that the porosity close to the wall became less than that in non-sintered porous media [22]. Therefore, the friction factor in the sintered porous media may be larger than that in non-sintered porous media. The following relation better predicts the friction factor in the sintered porous channel for larger particles:

$$f_e = \frac{117.9}{Re_e} + 0.63 \quad (\text{for } Re_e < 800). \tag{3}$$

This correlation was developed using a least square analysis of the present experimental data for particle diameters from 1.0 to 2.0 mm.

3.2. Heat transfer coefficients and heat transfer enhancement

Figs. 5 and 6 show the distribution of the local heat transfer coefficients for convection heat transfer of water and air in the sintered bronze porous plate channels and the calculated results in the empty plate channel. The local heat-transfer coefficients increased with Reynolds number and decreased along the axial direction except near the outlet section where the heat transfer increased due to the exit effect. The porous media greatly increased the heat transfer coefficient compared to the empty channel. For the sintered bronze packed beds, the local heat transfer coefficient was enhanced 5–15 times for water and 6–30 times for air depending on the mass flow rate. The influence of Reynolds number (or flow rate) on the local convection heat transfer coefficient for air in the sintered porous media was much stronger than for water as will be discussed later.

Fig. 7 compares the local heat transfer coefficients at the middle of the test section for convection heat transfer of water and air in the sintered bronze porous plate channels with those in an empty plate channel. The local heat transfer coefficients at the middle of the test section increased as the Reynolds number increased. The heat transfer coefficients can be related to the equivalent Reynolds number by

$$Nu = aRe_D^b \quad (\text{for } Re_D < 8000). \tag{4}$$

The values of a and b in Eq. (4) for the different fluids and particle diameters determined using a least square analysis of the present experimental data are listed in Table 1. The deviation between Eq. (4) and the experimental data was less than 10%.

The porous media greatly increased the heat transfer coefficient for both water and air compared to the empty channel. Table 2 presents the ratios by which the heat transfer was enhanced in the sintered porous plate channels compared to an empty channel. For these conditions, the sintered bronze porous media enhanced the average heat transfer coefficient 7–14 times for water and 3–36 times for air depending on the mass flow rate.

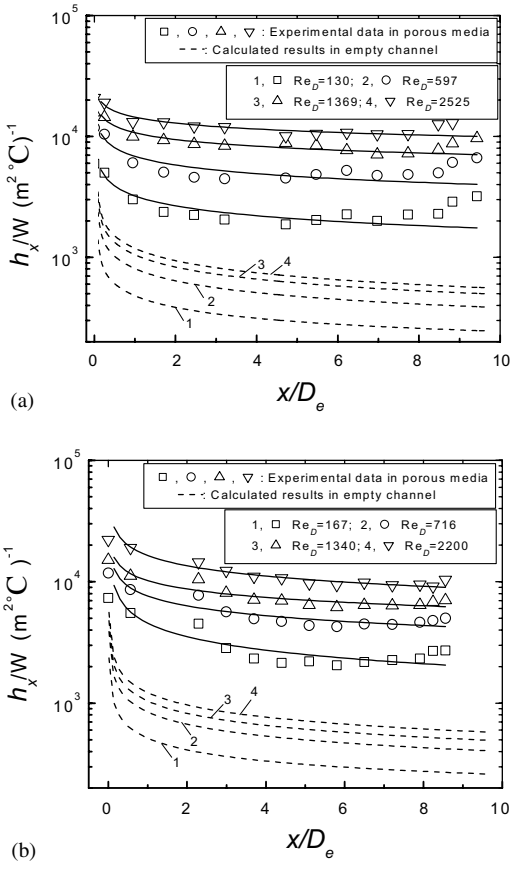

Fig. 5. Local heat transfer coefficient for water in sintered porous plate channels: (a) $d_p = 1.0$–1.4 mm and (b) $d_p = 0.5$–0.71 mm.

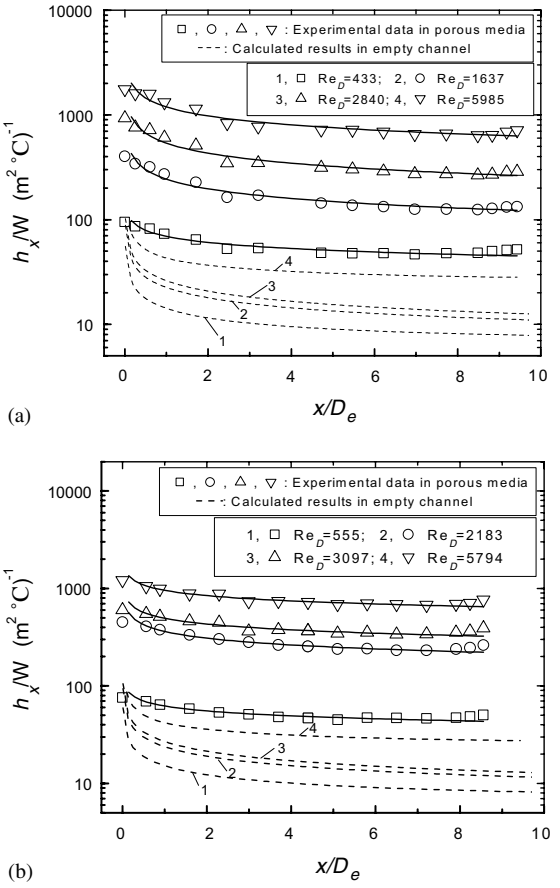

Fig. 6. Local heat transfer coefficient for air in sintered porous plate channels: (a) $d_p = 1.0$–1.4 mm and (b) $d_p = 0.5$–0.71 mm.

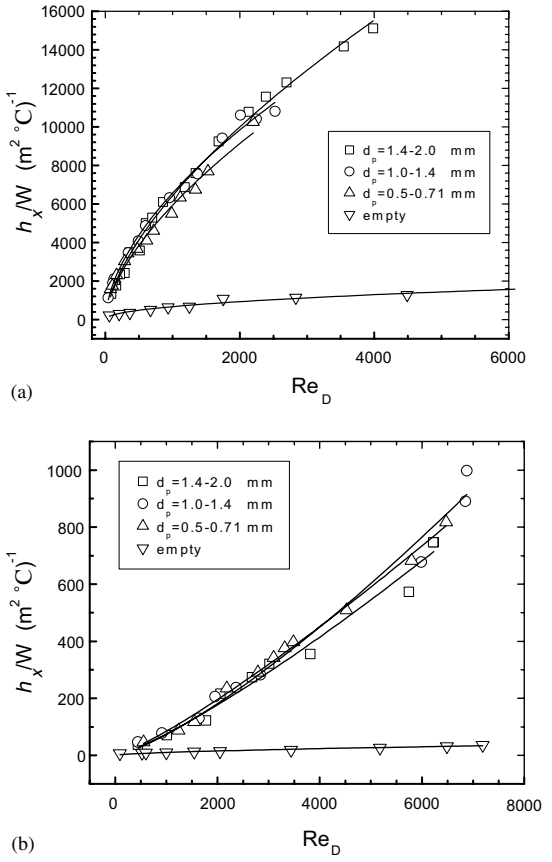

Fig. 7. Local heat transfer coefficients at the middle of the test section for water (a) and air (b) in sintered porous plate channels and in the empty plate channel. □, ○, △, ▽ experimental results; — curve fit of the experimental data.

Table 1
Values of a and b in Eq. (4) for different fluids and particle diameters

Particle diameter (mm)	1.4–2.0	1.0–1.4	0.5–0.71	Empty channel
Water				
a	79.37662	116.5744	80.56446	25.8906
b	0.63627	0.58361	0.62241	0.47124
Air				
a	0.0156	0.00868	0.02101	0.15604
b	1.22832	1.30883	1.20259	0.60525

The results in Table 2 show that the heat transfer enhancement in the sintered porous media for air increased sharply with increasing flow rate, while the heat transfer enhancement in the sintered porous media for water increased gradually with increasing flow rate. Table 1 shows that the exponents b in Eq. (4) for convection heat transfer of water in sintered porous media and in empty channel were similar, while for convection heat transfer of air in sintered porous media the exponents b in Eq. (4) were much larger than that in the empty channel.

The different influences of the flow rate on the convection heat transfer for water and air in sintered porous media are caused by their different heat transfer mechanisms in porous media. Jiang et al. [8] showed that convection heat transfer in porous plate channels is controlled by two factors, the convection heat transfer between the fluid and the channel surface, and the "fin effect" of the particles which intensifies with increasing particle thermal conductivity and Reynolds number. The "fin effect" of the particles is controlled by the combined effects of the convection heat transfer between the fluid and the particles and the thermal conduction between the particles. For sintered metallic porous media, the porosity at the wall and the thermal contact resistance are less than with non-sintered porous media; therefore, the heat transport from the wall to the interior of the porous media is more intense for sintered metallic porous media which enhances the overall heat transfer coefficient at the wall. For convection heat transfer of air in sintered porous media, the sintered bronze particles transfer much more heat from the upper surface to the volume than is transferred by the air in the porous media, so the overall heat transfer intensity is mainly limited by the convection heat transfer from the porous media to the air. Therefore, the convection heat transfer enhancement for air in the sintered porous channel increases sharply with increasing flow rate (or Reynolds number). However, for water, the heat transfer mechanism is quite different since the heat transfer capability of water is much greater. The overall heat transfer rate with water depends on both of the convection heat transfer within the water and the heat transfer through the sintered porous media into the interior. Therefore, the increases in the convection heat transfer coefficients for water in the sintered porous channel were not as great with variations of the flow rate as for air.

3.3. Effect of particle diameter on the heat transfer

The results in Fig. 7 show that for the conditions studied here, the influence of the particle diameter on the convection heat transfer of water and air in sintered porous media was not very great. Jiang et al. [8] presented a criterion for determining how the convection heat transfer coefficients in non-sintered porous media vary with particle diameter. They found that if $\rho_0 u_0 d_p > 0.065\lambda_f^{-4.82}\lambda_m^{5.82}/c_{pf}(\varepsilon_m/(1-\varepsilon_m))$, then the convection heat transfer coefficient will increase with increasing particle diameter. According to this criterion, for water in these porous media, the diameter particle

Table 2
Heat transfer enhancement in sintered porous media

Fluid	Particle diameter (mm)	Re_D					
		200	500	1000	2000	5000	10,000
Water	1.4–2.0	7.35	8.55	9.59	10.75	12.50	14.02
	1.0–1.4	8.17	9.05	9.79	10.58	11.73	12.67
	0.5–0.71	6.93	7.96	8.84	9.82	11.28	12.52
Air	1.4–2.0	2.71	4.80	7.40	11.39	20.17	31.06
	1.0–1.4	2.31	4.41	7.18	11.69	22.27	36.27
	0.5–0.71	3.19	5.51	8.34	12.62	21.81	33.00

should have little effect on the convection heat transfer coefficient of water in the sintered porous media; while the convection heat transfer coefficient of air in the sintered porous media should increase with decreasing particle diameter. However, the results in Fig. 7 and Table 2 show that this criterion is unsuitable for sintered porous media. In fact, the effect of solid particle diameter on the convection heat transfer is quite complicated. More detailed analysis and experimental results describing the effect of particle diameter on the heat transfer in sintered porous media are needed to completely understand the effect.

3.4. Comparison of convection heat transfer in sintered and non-sintered porous media

The main differences between sintered and non-sintered porous media are that for the sintered metallic porous media, the porosity near the wall and the thermal contact resistances between the particles and between the particles and the wall surface are less than in non-sintered porous media due to fusing in the sintering process which not only increases the molecular contact between surfaces but also increases the contact surface areas. Therefore, the effective thermal conductivity of the sintered solid phase will be much higher than that of non-sintered packed beds, and the heat transport from the wall to the interior of the porous media will be greater for sintered metallic porous media, which will enhance the overall heat transfer coefficient at the wall.

According to Achenbach [23], the convection heat transfer at the wall for fluid flow in a horizontal porous plate channel can be expressed as:

$$Nu_w = \left(1 - \frac{d_p}{D_e}\right) Re_D^{0.61} Pr^{1/3} \quad (100 < Re_D < 2 \times 10^4). \tag{5}$$

Nu_w at the wall for convection heat transfer in a horizontal porous plate channel depends on three parameters including d_p/D_e, Re_D and Pr. The convection heat transfer at the wall in porous channels also depends on the particle thermal conductivity. For the similar particle thermal conductivities, the heat transfer rates can be compared for similar conditions including d_p/D_e, Re_D and Pr.

The convection heat transfer rates in sintered and non-sintered porous media were compared using the following experimental conditions: for water in a sintered bronze porous plate channel, $d_p = 0.605$ mm and $D_e = 21.4$ mm, while in a non-sintered bronze porous plate channel, $d_p = 0.278$ mm and $D_e = 9.41$ mm; for air in a sintered bronze porous plate channel, $d_p = 1.2$ mm and $D_e = 19.9$ mm, while in a non-sintered steel porous plate channel, $d_p = 1.2$ mm and $D_e = 18.2$ mm. The experimental data for water and air in sintered porous media is from the present work, the experimental data for water in non-sintered porous media is from Jiang et al. [8], while the experimental data for air in non-sintered porous media is from Jiang et al. [9]. The data sets have similar values of the similarity variables.

Fig. 8 presents experimental data for the local Nusselt numbers of water and air in sintered and non-sintered porous plate channels. The data shows that the convection heat transfer of air in the sintered porous plate channel is much higher than in the non-sintered porous media. The difference for convection heat transfer of water in sintered and non-sintered porous plate channels was not as large as for air.

Fig. 9 presents experimental data for the average Nusselt number for water and air in sintered and non-sintered porous plate channels, and in an empty channel. The dimensionless length, L/D_e, for the present data for the sintered porous channel is larger than for the data for the non-sintered packed beds [8,9]; therefore, the average Nusselt number in the sintered porous channel were recalculated using the same L/D_e as in the non-sintered packed beds. The results show that the average Nusselt number for water and air in the sintered porous plate channel is larger than for the non-sintered porous media, especially for air. Experimental research on convection heat transfer of air in non-sintered porous media [9] showed that the heat transfer enhancement by the non-sintered porous media was not large (only 5-fold) because the thermal contact resistance between the particles and between the particles and the wall with air

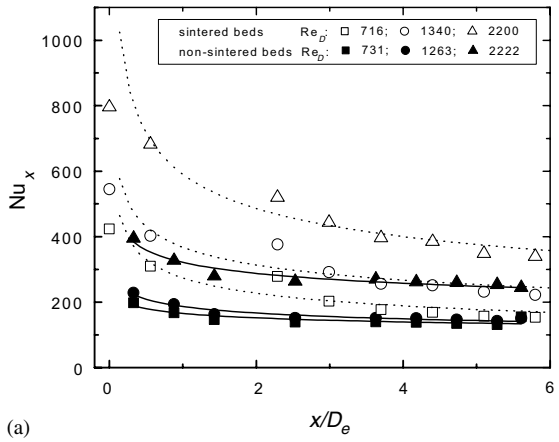

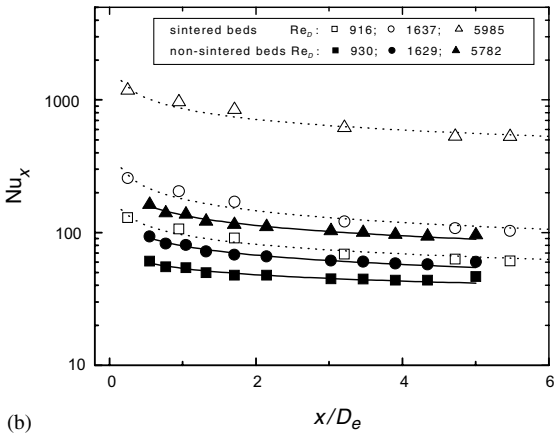

Fig. 8. Local Nusselt number for water (a) and air (b) in sintered and non-sintered porous media.

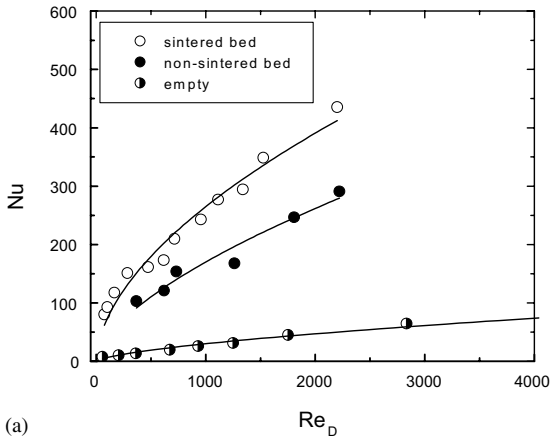

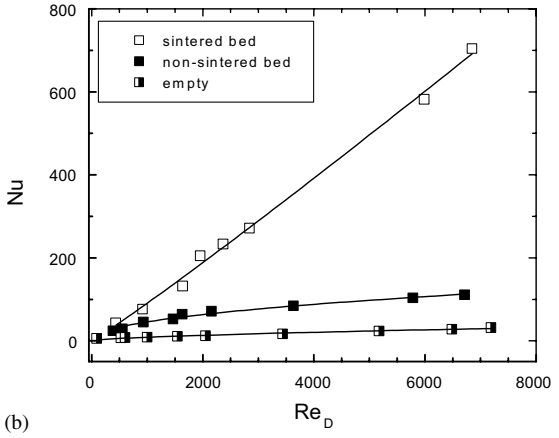

Fig. 9. Average Nusselt number for water (a) and air (b) in sintered and non-sintered porous media.

in the non-sintered porous media was relatively large and because the contact surface area between the particles and the wall was relatively small for non-sintered porous media. Therefore, sintered porous media provide much more heat transfer enhancement than non-sintered packed beds, especially for low thermal conductivity fluids.

3.5. Effective thermal conductivity of sintered and non-sintered porous media

In Section 3.4, the higher heat transfer coefficient in sintered porous media compared to non-sintered packed beds was attributed to the better thermal conductivity of the sintered solid phase. To prove this point, the effective thermal conductivities of the sintered and non-sintered porous media were measured experimentally.

The plane-heat-source method was used to measure the effective thermal conductivity of the porous media. A constant heat flux was applied to the upper surface of the porous plate, while the bottom surface of the plate channel was cooled by water with a large flow rate to keep a constant bottom surface temperature. The surroundings were well insulated. The average temperatures of the upper surface, t_u, and the bottom surface, t_l, were measured by thermocouples. The heat flux measurement method was the same as described in Section 2. The effective thermal conductivity of the porous media was calculated using

$$\lambda_m = \frac{q_w \cdot h_c}{t_u - t_l}. \quad (6)$$

Three sintered porous plates with different particle diameters and one non-sintered packed bed were tested. The experimental results are listed in Table 3. A detailed analysis estimated the experimental uncertainty in the effective thermal conductivity of the porous media to be ±10.3%.

The data in Table 3 shows that for the 0.5–0.7 mm diameter particles, the experimental data for non-sin-

Table 3
Effective thermal conductivity of sintered and non-sintered porous media

Type of porous media	d_p [mm]	λ_m [W/(m °C)]		
		Experimental data	Correlation for non-sintered [24]	$\lambda_s \cdot (1-\varepsilon_m)$
Sintered	1.4–2.0	2.012	0.348	29.0
Sintered	1.0–1.4	2.865	0.378	30.0
Sintered	0.5–0.71	3.411	0.453	32.3
Non-sintered	0.5–0.7	0.798	0.606	35.8

tered porous media agrees well with the equation recommended by Zehner and Schlunder [24] for the effective thermal conductivity of non-sintered porous media, while the experimental results for the effective thermal conductivity of the sintered porous plate were much larger (4 times). Therefore, the sintering process significantly improved the thermal contact between the particles and between the particles and the wall, which enhanced the effective thermal conductivity. The effective thermal conductivities of the porous media calculated using $\lambda_s \cdot (1-\varepsilon_m)$ are much higher than the experimental data. Table 3 shows that the effective thermal conductivity of the sintered porous plate channel with smaller particles was larger than that with larger particles probably due to the lower porosity with the smaller particles.

4. Conclusions

(1) The sintered porous media greatly increased the heat transfer coefficient. For the conditions in this paper, the sintered bronze porous media enhanced the local heat transfer coefficient 15-fold for water and up to 30-fold for air depending on the mass flow rate.

(2) The heat transfer enhancement due to the sintered porous media with air increased sharply with increasing flow rate, while the heat transfer enhancement due to the sintered porous media with water increased gradually with increasing flow rate.

(3) For the conditions studied here, the particle diameter had little effect on the convection heat transfer in sintered porous media.

(4) The convection heat transfer in the sintered porous plate channels was higher than in non-sintered porous plate channels due to the reduced thermal contact resistance and the reduced porosity at the wall in the sintered channels. The difference between the convection heat transfer in sintered and non-sintered porous media for air was much larger than for water.

(5) The effective thermal conductivity of the sintered porous media was found to be much higher than for non-sintered porous media due to the improved thermal contact caused by the sintering process.

Acknowledgements

The project was supported by the National Outstanding Youth Fund from the National Natural Science Foundation of China (No. 50025617) and the Major State Basic Research Development Program (No. G1999033106). We also thank Dr. David Christopher for editing the English.

References

[1] V.I. Subbojin, V.V. Haritonov, Thermophysics of cooled laser mirrors, Teplofizika Vys. Temp. 29 (2) (1991) 365–375 (in Russian).
[2] U.A. Jeigarnik, F.P. Ivanov, N.P. Ikranikov, Experimental data on heat transfer and hydraulic resistance in unregulated porous structures, Teploenergetika (2) (1991) 33–38 (in Russian).
[3] J.L. Lage, A.K. Weinert, D.C. Price, R.M. Weber, Numerical study of a low permeability microporous heat sink for cooling phased-array radar systems, Int. J. Heat Mass Transfer 39 (17) (1996) 3633–3647.
[4] G.M. Chrysler, R.E. Simons, An experimental investigation of the forced convection heat transfer characteristics of fluorocarbon liquid flowing through a packed-bed for immersion cooling of microelectronic heat sources, in: AIAA/ASME Thermophysics and Heat Transfer Conference, Cryogenic and Immersion Cooling of Optics and Electronic Equipment, ASME HTD-131, 1990, pp. 21–27.
[5] S.M. Kuo, C.L. Tien, Heat transfer augmentation in a foam-material filled duct with discrete heat sources, in: Intersociety Conference on Thermal Phenomena in the Fabrication and Operation of Electronic Components, IEEE, New York, 1988, pp. 87–91.
[6] G.J. Hwang, C.H. Chao, Heat transfer measurement and analysis for sintered porous channels, J. Heat Transfer 116 (1994) 456–464.
[7] P.X. Jiang, Z.P. Ren, B.X. Wang, Numerical simulation of forced convection heat transfer in porous plate channels using thermal equilibrium and nonthermal equilibrium models, Numer. Heat Transfer, Part A 35 (1999) 99–113.
[8] P.X. Jiang, Z. Wang, Z.P. Ren, B.X. Wang, Experimental research of fluid flow and convection heat transfer in porous plate channels filled with glass or metallic particles, Exp. Thermal Fluid Sci. 20 (1999) 45–54.
[9] P.X. Jiang, G.S. Si, M. Li, Z.P. Ren, Forced convection heat transfer of air in a porous plate channel, in:

Proceedings of the 5th Beijing International Conference on Heat Transfer, Beijing, August 6–10, 2000, pp. 492–497.
[10] K. Khanafer, K. Vafai, Isothermal surface production and regulation for high heat flux application utilizing porous inserts, Int. J. Heat Mass Transfer 44 (2001) 2933–2947.
[11] K. Vafai, C.L. Tien, Boundary and inertial effects on flow and heat transfer in porous media, Int. J. Heat Mass Transfer 24 (1981) 195–203.
[12] A. Narasimhan, J.L. Lage, D.A. Nield, D.C. Porneala, Experimental verification of two new theories predicting temperature-dependent viscosity effects on the forced convection in a porous channel, J. Heat Transfer 123 (2001) 948–951.
[13] A. Narasimhan, J.L. Lage, D.A. Nield, New theory for forced convection through porous media by fluids with temperature-dependent viscosity, J. Heat Transfer 123 (2001) 1045–1051.
[14] P.X. Jiang, M. Li, Z.P. Ren, Forced convection heat transfer in plate channels filled with packed beds or sintered porous media, Tsinghua Sci. Technol. 7 (2) (2002) 202–208.
[15] A. Amiri, K. Vafai, T.M. Kuzay, Effects of boundary conditions on non-Darcian heat transfer through porous media and experimental comparisons, Numer. Heat Transfer, Part A 27 (1995) 651–664.
[16] M. Quintard, Modelling local non-equilibrium heat transfer in porous media, in: Heat Transfer 1998, Proceedings of 11th International Heat Transfer Conference, Kyongju, Korea, vol. 1, 1998, pp. 279–285.
[17] D.Y. Lee, K. Vafai, Analytical characterization and conceptual assessment of solid and fluid temperature differences in porous media, Int. J. Heat Mass Transfer 42 (1999) 423–435.
[18] P.X. Jiang, Z.P. Ren, Numerical investigation of forced convection heat transfer in porous media using a thermal non-equilibrium model, Int. J. Heat Fluid Flow 22 (1) (2001) 102–110.
[19] B. Alazmi, K. Vafai, Constant wall heat flux boundary conditions in porous media under local thermal non-equilibrium conditions, Int. J. Heat Mass Transfer 45 (2002) 3071–3087.
[20] B.S. Petukhov, L.G. Genin, S.A. Kovalev, Heat Transfer in Nuclear Power Equipment, Energoatomizdat Press, Moscow, 1986 (in Russian).
[21] M.E. Aerov, O.M. Tojec, Hydraulic and Thermal Basis on the Performance of Apparatus with Stationary and Boiling Ganular Layer, Himia Press, Leningrad, 1968 (in Russian).
[22] P.X. Jiang, M. Li, Y.C. Ma, Z.P. Ren, Boundary conditions and wall effect for forced convection heat transfer in sintered porous plate channels, Int. J. Heat Mass Transfer, in press.
[23] E. Achenbach, Heat and flow characteristics of packed beds, Exp. Thermal Fluid Sci. 10 (1995) 17–27.
[24] P. Zehner, E.U. Schlunder, Thermal conductivity of granular materials at moderate temperature, Chem. Ing. Tech. 42 (1970) 933–941.